

Anharmonic phonon frequency shift in MgB₂

Michele Lazzeri, Matteo Calandra, and Francesco Mauri

Laboratoire de Minéralogie-Cristallographie de Paris, 4 Place Jussieu, 75252, Paris cedex 05, France

(Dated: October 23, 2018)

We compute the anharmonic shift of the phonon frequencies in MgB₂, using density functional theory. We explicitly take into account the scattering between different phonon modes at different q-points in the Brillouin zone. The shift of the E_{2g} mode at the Γ point is +5% of the harmonic frequency. This result comes from the cancellation between the contributions of the four- and three-phonon scattering, respectively +10% and -5%. A similar shift is predicted at the A point, in agreement with inelastic X-ray scattering phonon-dispersion measurements. A smaller shift is observed at the M point.

PACS numbers: 63.20.Dj, 63.20.Kr, 71.15.Mb

The discovery of high critical temperature ($T_c = 39\text{K}$) in MgB₂ [1] has challenged our understanding of electron-phonon coupling mediated superconductivity. Several mechanisms might cooperate in determining the actual value of T_c in MgB₂, including the existence of a double gap structure [2, 3, 4], and anharmonic effects [5, 6, 7, 8, 9, 10]. Much attention has been devoted to the study of the E_{2g} phonon mode, which consists of an antiphase vibration of the two boron atoms, parallel to the hexagon plane. This mode has the largest coupling with electrons according to inelastic X-ray scattering measurements [11], in agreement with a commonly accepted interpretation of the MgB₂ electronic band structure [5, 12, 13]. The E_{2g} mode has also been associated with a supposedly large anharmonicity, but a quantitative determinations of the anharmonic effects has led so far to controversial results [5, 6, 7, 8, 9, 10, 11].

In particular, actual theoretical calculations indicate the anharmonic frequency shift of the E_{2g} mode at Γ to be large, with varying estimates that range from +15% [5, 6], up to +20/25% [7, 9] of the theoretical harmonic frequency (~ 65 meV). A comparably large shift is expected to affect this mode all along the Γ -A direction [5, 6]. Raman measurements [14, 15, 16, 17] seem to confirm the prediction of a large anharmonicity at Γ . In fact, the best resolved spectra [16], present a peak at 77 meV (*i.e.* 18% higher than the harmonic frequency) that could be attributed to the E_{2g} mode at Γ . However, the structure observed below 40 meV [16], and the clearly asymmetric profile (reminiscent of a Fano resonance) of the 77 meV peak indicate that the Raman experiment probes not just phonon vibrations, but electronic excitations as well. Thus, the position of the 77 meV peak does not necessarily correspond to the E_{2g} phonon frequency. Moreover, Raman spectra display a drastic dependence on the temperature. The width of the 77 meV peak is ~ 20 meV at $T=40\text{K}$ and reaches almost 40 meV at room temperature [16, 17]. This behavior has been tentatively attributed to anharmonicity [16, 17], but, according to the calculations of Ref. [11], the E_{2g}- Γ anharmonic broadening at room temperature is negligible, just 1.2 meV.

The determination of the phonon frequency from Raman data requires further analysis, as suggested in Ref. [16], together with a clear understanding of the temperature dependence.

On the other hand, the prediction of a strong anharmonic frequency shift is in stark contrast with the inelastic X-ray measurements of the MgB₂ phonon dispersion of Ref. [11], which E_{2g} phonon frequencies measurements are in agreement (within 5%) with the calculated harmonic phonon frequencies [11, 13, 14] at several points along the Γ -A direction. Contrary to Raman scattering [16, 17], in X-ray inelastic scattering the cross-section of electronic excitations is much smaller than that of the phonon excitations. Thus, X-ray measurements are a direct probe of the phonon frequencies. Small anharmonic frequency shift is also suggested by a recent point-contact spectroscopy measurement [18].

The origin of the discrepancy between the predicted large anharmonic shift of the E_{2g} mode [5, 6, 7, 8, 9, 10] and the inelastic X-ray scattering measurements [11], might be traced back to the approximations involved in the calculations. We recall here that the anharmonic frequency shift of a phonon mode ($\mathbf{q}j$) (identified by the reciprocal-space vector \mathbf{q} and by the band index j) is due to the anharmonic interaction with the ensemble of all phonons, having different momentum \mathbf{q} and different j . Up to now, theoretical studies of MgB₂ have been based on the study of a frozen-phonon energy profile. This approach completely neglects: (i) the dependence of the anharmonic scattering on the exchanged phonon momentum \mathbf{q} , and (ii) the coupling between phonons having different j . The calculation of the anharmonic scattering between phonons having different \mathbf{q} and different j is possible, using first-principles [20] techniques. *E.g.*, it has allowed the determination of anharmonic line shift and broadening of the Raman modes in covalent semiconductors [19]. However, this approach is computationally demanding and has not been yet applied to MgB₂.

In this Letter we compute the anharmonic frequency shift of the phonon E_{2g} mode of MgB₂ from first-

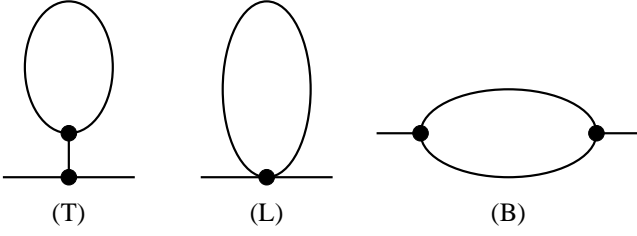


FIG. 1: Diagrammatic representation of the leading terms in the perturbative expansion of a non-harmonic phonon Hamiltonian (see the text).

principles [20]. We explicitly take into account the scattering between different phonon modes at different \mathbf{q} -points in the reciprocal space. We use the density-functional perturbation theory of Ref. [21]. The anharmonic terms of the phonon Hamiltonian are obtained using a method, based on the “ $2n + 1$ ” theorem, which allows the efficient calculation of third order derivatives of total energy, at any point in the reciprocal space, in metallic systems [22].

The phonon excitations of a crystal are determined by the interatomic energy, and correspond to the poles of the interacting phonon Green function [23, 24]. $\Pi_{\mathbf{q}j}(\omega)$ represents the anharmonic contribution to the phonon self-energy of the phonon mode ($\mathbf{q}j$) having frequency $\omega_{\mathbf{q}j}$. In the case $|\Pi_{\mathbf{q}j}| \ll \omega_{\mathbf{q}j}$, the frequency shift $\Delta_{\mathbf{q}j}$ and line broadening $\Gamma_{\mathbf{q}j}$, can be obtained as $\Delta_{\mathbf{q}j} = \mathcal{R}_e[\Pi_{\mathbf{q}j}(\omega_{\mathbf{q}j})]$

and $\Gamma_{\mathbf{q}j} = -\mathcal{I}_m[\Pi_{\mathbf{q}j}(\omega_{\mathbf{q}j})]$, \mathcal{R}_e and \mathcal{I}_m being the real and imaginary part of a complex number. The three lowest order terms in the perturbative expansion, for a fixed cell geometry, are:

$$\Pi_{\mathbf{q}j}(\omega) = \Pi_{\mathbf{q}j}^{(T)}(\omega) + \Pi_{\mathbf{q}j}^{(L)}(\omega) + \Pi_{\mathbf{q}j}^{(B)}(\omega), \quad (1)$$

which correspond, respectively, to the tadpole (T), loop (L), and bubble (B) diagrams of Fig. 1, whose calculation is described in *e.g.* in Refs. [23, 24].

Let us consider the interatomic potential energy $\mathcal{E}^{tot}(\{u_{s\alpha}(\mathbf{R}_i)\})$, where $u_{s\alpha}(\mathbf{R}_i)$ is the displacement from the equilibrium position of the s -th atom in the crystal cell identified by the lattice vector \mathbf{R}_i along the α Cartesian coordinate. We define

$$V^{(n)}(\mathbf{q}_1j_1, \dots, \mathbf{q}_nj_n) = \frac{\partial^n \mathcal{E}^{cell}}{\partial u_{\mathbf{q}_1j_1} \dots \partial u_{\mathbf{q}_nj_n}},$$

where \mathcal{E}^{cell} is the energy per unit cell and the adimensional quantity $u_{\mathbf{q}j}$ is defined by $u_{\mathbf{q}j} = \frac{1}{N} \sum_{i,s,\alpha} \sqrt{\frac{2M_s\omega_{\mathbf{q}j}}{\hbar}} v_{s\alpha}(\mathbf{q}j) u_{s\alpha}(\mathbf{R}_i) e^{-i\mathbf{q}\cdot\mathbf{R}_i}$, $v_{s\alpha}(\mathbf{q}j)$ being the orthogonal phonon eigenmodes normalized on the unit cell, M_s the atomic mass, and N the number of \mathbf{q} -points describing the system (or unit cells). Using this definition $V^{(n)}$ is a intensive quantity, independent of N , at any order n . The evaluation of the three diagrams for the j zone center mode ($\mathbf{q} = \mathbf{0}$) yields:

$$\begin{aligned} \Pi_{\mathbf{0}j}^{(T)}(\omega) &= -\frac{1}{N\hbar^2} \sum_{\mathbf{q},j_1,j_2} \frac{V^{(3)}(\mathbf{0}j, \mathbf{0}j, \mathbf{0}j_1) V^{(3)}(\mathbf{0}j_1, -\mathbf{q}j_2, \mathbf{q}j_2)}{\omega_{\mathbf{0}j_1}} (2n_{\mathbf{q}j_2} + 1) \\ \Pi_{\mathbf{0}j}^{(L)}(\omega) &= \frac{1}{2N\hbar} \sum_{\mathbf{q},j_1} V^{(4)}(\mathbf{0}j, \mathbf{0}j, -\mathbf{q}j_1, \mathbf{q}j_1) (2n_{\mathbf{q}j_1} + 1) \\ \Pi_{\mathbf{0}j}^{(B)}(\omega) &= -\frac{1}{2N\hbar^2} \sum_{\mathbf{q},j_1,j_2} |V^{(3)}(\mathbf{0}j, -\mathbf{q}j_1, \mathbf{q}j_2)|^2 \left(\frac{2(\omega_{\mathbf{q}j_1} + \omega_{\mathbf{q}j_2})(1 + n_{\mathbf{q}j_1} + n_{\mathbf{q}j_2})}{(\omega_{\mathbf{q}j_1} + \omega_{\mathbf{q}j_2})^2 - (\omega + i\delta)^2} + \frac{2(\omega_{\mathbf{q}j_1} - \omega_{\mathbf{q}j_2})(n_{\mathbf{q}j_2} - n_{\mathbf{q}j_1})}{(\omega_{\mathbf{q}j_2} - \omega_{\mathbf{q}j_1})^2 - (\omega + i\delta)^2} \right), \end{aligned} \quad (2)$$

where $\sum_{\mathbf{q}}$ is a sum on the Brillouin zone (BZ), $n_{\mathbf{q}j}$ is the Bose-statistics occupation of the phonon mode ($\mathbf{q}j$), and δ is a small positive number. Interpreting the three diagrams of Fig. 1 in terms of scattering between phonons, the self-energy $\Pi_{\mathbf{q}j}(\omega)$ can thus be expressed as a sum, over the BZ, of the phonon scattering coefficients $V^{(n)}$.

Eqs. 1,2 are valid at fixed cell geometry. In general, the dependence of $\Pi_{\mathbf{q}j}(\omega)$ on the temperature depends on further terms related to the thermal expansion of the lattice. However, if one can determine the lattice thermal expansion independently (*e.g.* experimentally), the shift at a given temperature can be obtained computing

the harmonic frequency at the lattice parameters corresponding to that temperature. While only the $\Pi^{(B)}$ term in Eq. 1 has an imaginary component (*i.e.* is providing a contribution to the line broadening, which we already calculated and discussed in Ref. [11]), all three diagrams have real part and contribute to the shift. Due symmetry, the $\Pi^{(T)}$ term is zero [25] in MgB_2 , and the frequency shift can, thus, be decomposed in three- and four-phonon scattering contributions $\Delta_{\mathbf{0},j}^{(3)} = \mathcal{R}_e[\Pi_{\mathbf{0},j}^{(B)}(\omega_{\mathbf{0}j})]$ and $\Delta_{\mathbf{0},j}^{(4)} = \mathcal{R}_e[\Pi_{\mathbf{0},j}^{(L)}(\omega_{\mathbf{0}j})]$.

Several authors used the frozen-phonon approach to

$\Delta_{ND}^{(4)}$	$\Delta^{(4)}$	$\Delta^{(3)}$	Δ^{tot}
T = 0 K, $\omega = 65.14$ meV			
9.46 (+15%)	6.00 (+9.2%)	-2.88 (-4.4%)	3.12 (+4.8%)
8.91 (+14%)	7.18 (+11%)	-2.99 (-4.6%)	4.19 (+6.4%)
T = 300 K, $\omega = 64.51$ meV			
10.68 (+16%)	6.52 (+10%)	-3.03 (-4.7%)	3.50 (+5.4%)
10.01 (+15%)	7.77 (+12%)	-3.12 (-4.8%)	4.65 (+7.2%)

TABLE I: Phonon frequency shift (meV) of the E_{2g} mode at the BZ center (Γ point). $\Delta^{(3)}$ ($\Delta^{(4)}$) is the shift due to the three(four)-phonon scattering contribution. Δ^{tot} ($\Delta^{tot} = \Delta^{(3)} + \Delta^{(4)}$) is the total shift. $\Delta_{ND}^{(4)}$ is defined in the text. ω is the unperturbed phonon frequency, and the values in parentheses are the shift as a percentage with respect to the ω at the corresponding temperature (T). Bold face values are obtained using the $16 \times 16 \times 16$ electronic integration grid, the others from a less converged $14 \times 14 \times 8$ grid [31].

determine MgB_2 frequency shift [5, 6, 7, 8, 9]. This approach is based on the study of the energy profile $\mathcal{E}_{\mathbf{q}=0,j}(\lambda)$ obtained displacing MgB_2 atomic positions by a value proportional to λ , along the eigenvector of mode j at $\mathbf{q} = 0$. This approach is valid when: (i) the coupling of the mode j with different modes is negligible; (ii) the anharmonic interaction does not change over the BZ, *i.e.* when $V^{(n)}(\mathbf{0}j, \mathbf{q}_2j, \dots, \mathbf{q}_nj) \sim V^{(n)}(\mathbf{0}j, \mathbf{0}j, \dots, \mathbf{0}j) \quad \forall \mathbf{q}_2, \dots, \mathbf{q}_n \in \text{BZ}$. Only in this non-dispersive regime the behavior of $\mathcal{E}_{\mathbf{q}=0,j}(\lambda)$ gives quantitative informations about the shift.

Our electronic structure calculations is performed using a plane-wave basis set up to a 35 Ry cutoff, and using the pseudopotential approach [26]. The terms $V^{(3)}$ of Eq. 2 are computed analytically with the approach of Ref. [22] and the $V^{(4)}$ are obtained by finite differentiation of $V^{(3)}$. Calculations are repeated both at T=0 K and T=300 K temperature crystal structures [27]. First order Hermite-Gaussian smearing of 0.025 Ry is used. The dynamical matrices and phonon frequencies are calculated using the PBE [29] approximation for the exchange and correlation functional and a well converged $16 \times 16 \times 16$ Monkhorst-Pack grid for the electronic BZ integration. Due to the actual implementation in our code, third and fourth order interatomic force constants ($V^{(3)}$ and $V^{(4)}$) are obtained using the LDA [30] functional. By performing frozen-phonon calculations at Γ using both PBE and LDA we estimate that the total shift obtained by LDA should be slightly larger ($\lesssim 0.5$ meV) than with PBE.

In Tab. I we show the computed values of $\Delta^{(4)}$ and $\Delta^{(3)}$ (previously defined) for the E_{2g} mode at Γ . To

	ω	$\Delta^{(4)}$	$\Delta^{(3)}$	Δ^{tot}
T = 0 K				
Γ, E_{2g}	65.14	7.18	-2.99	4.19 (+6.4%)
A (E_{2g})	57.50	7.77	-3.10	4.67 (+8.1%)
M (E_{2g})	87.18	4.12	-1.98	2.13 (+2.4%)
M (E_{2g})	93.10	1.10	-1.29	-0.19 (-0.2%)
Γ, E_{1u}	40.03	0.48	-0.24	0.25 (+0.6%)
Γ, A_{2u}	46.21	1.45	-0.36	1.09 (+2.4%)
Γ, B_{1g}	84.49	-1.02	-0.16	-1.18 (-1.4%)
T = 300 K				
Γ, E_{2g}	64.51	7.77	-3.12	4.65 (+7.2%)
A (E_{2g})	56.88	8.16	-3.50	4.66 (+8.2%)
M (E_{2g})	86.65	4.65	-2.13	2.52 (+2.9%)
M (E_{2g})	92.80	1.20	-1.46	-0.26 (-0.3%)
Γ, E_{1u}	39.74	0.76	-0.30	0.46 (+1.2%)
Γ, A_{2u}	45.81	0.20	-0.64	-0.45 (-1.0%)
Γ, B_{1g}	84.28	-1.03	-0.21	-1.24 (-1.5%)

TABLE II: Phonon frequency shift (meV) of various modes at the three high symmetry points Γ , A, and M of the BZ (see also the caption of Tab. I). The shifts of this table are obtained using the $14 \times 14 \times 8$ electronic integration grid [31].

make a comparison with the frozen-phonon approach, in Tab. I we also show $\Delta_{ND}^{(4)}$, namely the shift due to the four-phonon scattering obtained neglecting the interaction with the other modes, and assuming a non-dispersive anharmonic potential: *i.e.* imposing in Eq. 2 $V^{(4)}(\mathbf{0}j, \mathbf{0}j, -\mathbf{q}j_1, \mathbf{q}j_1) = V^{(4)}(\mathbf{0}j, \mathbf{0}j, \mathbf{0}j, \mathbf{0}j)\delta_{j_1,j}$. As expected [5, 6, 7, 8, 10], $\Delta_{ND}^{(4)}$ gives a large positive shift (+16% of the unperturbed frequency at T=300K), which, however, is far from being a quantitative estimate of the shift. In fact, the actual determination of scattering processes all over the BZ, and the inclusion of the other modes ($j_1 \neq j$), reduces the value of the four-phonon shift ($\Delta^{(4)}$ in Tab. I) to just +10%. Furthermore, the inclusion of the $\Delta^{(3)}$ term (which has a negative sign) reduces the total shift to just +5.4%. The main reason of the negative sign of $\Delta^{(3)}$ is that the joint density of phonon states $\rho(\omega) = \sum_{\mathbf{q}, j_1, j_2} \delta(\omega - \omega_{\mathbf{q}j_1} - \omega_{\mathbf{q}j_2})$ is almost entirely (more than 90%) distributed above the frequency of the Γ - E_{2g} mode. This implies that, in the summation done to obtain $\mathcal{R}_e(\Pi^{(B)})$ from Eq. 2 at T=0, the largest part of the terms have a negative value.

To compute the shift at the A and M BZ points ($\mathbf{q} \neq \mathbf{0}$) we use, respectively, a $1 \times 1 \times 2$, and a $2 \times 2 \times 1$ super-cell. Due to the heavier computational effort required, $V^{(3)}$ and $V^{(4)}$ are calculated with less converged electronic integration grids equivalent to a $14 \times 14 \times 8$ grid for the $1 \times 1 \times 1$ cell [31]. From Tab. I one can infer that calculations with this grid provide a qualitative description of the system. In Tab. II we show the shift, at A and M, of the modes belonging to the E_{2g} band, and, at Γ , the shift of modes different than E_{2g} . It is apparent that

the total E_{2g} shifts at Γ and A are greater than both the E_{2g} shift at M, and the shift of the other modes at Γ . This is not surprising: it is related to the strong electron-phonon coupling of the E_{2g} mode along the Γ -A direction [5], and confirms one accepted interpretation of the MgB_2 electronic band structure [5, 13]. Moreover, the E_{2g} shift at Γ and A are very similar, being 4.65 and 4.66 meV (Tab. II), respectively, at room temperature. This confirms the predicted presence of a uniform shift along the Γ -A direction [5, 9].

Keeping in mind that our best estimate for the Γ shift is just +3.5 meV (*i.e.* +5.4% of the harmonic value, from Tab. I) we expect the anharmonic shift to be of the same order all along Γ -A. Such a value is compatible with the room temperature inelastic scattering X-ray measurements of Ref. [11]. The measured E_{2g} dispersion along the Γ -A direction, from Ref. [11], is in agreement with harmonic model calculations. Indeed, comparing the experimental E_{2g} frequency at A (59.0 meV) with our calculation, even including anharmonic effects ($56.88 + 4.66 = 61.5$ meV, using the $14 \times 14 \times 8$ grid) the agreement remains well within the experimental error-bar and the typical DFT error.

Finally, we notice that our calculations predict an almost negligible dependence of the E_{2g} - Γ frequency from the temperature (being $65.14 + 3.12 = 68.26$ meV at $T = 0\text{K}$, and $64.51 + 3.50 = 68.01$ meV at $T = 300\text{K}$). In fact, the largest part of this shift is due to the coupling with phonons having a Debye temperature larger than 300K ($\omega > 26$ meV).

In conclusion, we have obtained the anharmonic phonon frequency shift in MgB_2 using density functional theory. Two ingredients which turned out to be essential for a quantitative description of the anharmonic E_{2g} -mode frequency-shift are: (i) the explicit calculation of the scattering processes all over the BZ; (ii) the inclusion in the perturbative expansion of both the three- and four-phonon scattering contributions, which have opposite sign. The resulting phonon frequency shift at Γ is just +5.4% of the harmonic frequency, and is expected to be of the same order along the Γ -A direction, in agreement with inelastic X-ray scattering [11].

We are grateful to O.K.Andersen, J.Kortus, I.Mazin, H.J. Choi, K.M.Rabe, and A.Shukla for useful discussions. M.C. was supported by a Marie Curie Fellowship, contract No. IHP-HPMF-CT-2001-01185. Calculation were done at the IDRIS supercomputing centre (Orsay, France), using the PHONON code: <http://www.pwscf.org>.

-
- [1] J. Nagamatsu *et al.*, Nature (London) **410**, 63 (2001).
 [2] S.V. Shulga *et al.*, cond-mat/0103154.
 [3] A.A. Golubov *et al.*, J. Phys. Cond. Matt. **14**, 1353

- (2002).
 [4] H.J. Choi *et al.*, Nature (London) **418**, 758 (2002).
 [5] A.Y. Liu, I.I. Mazin and J. Kortus, Phys. Rev. Lett. **87**, 087005 (2001).
 [6] J. Kortus *et al.*, Phys. Rev. Lett. **86**, 4656 (2001).
 [7] T. Yildirim *et al.*, Phys. Rev. Lett. **87**, 37001 (2001).
 [8] K. Kunc *et al.*, J. Phys. Cond. Matt. **13**, 9945 (2001).
 [9] H.J. Choi *et al.*, Phys. Rev. B **66**, 020513 (2002).
 [10] L. Boeri *et al.*, Phys. Rev. B **65**, 214501 (2002).
 [11] A. Shukla *et al.*, Phys. Rev. Lett. **90**, 095506 (2003).
 [12] J.M. An, and W.E. Pickett, Phys. Rev. Lett. **86**, 4366 (2001).
 [13] Y. Kong *et al.*, Phys. Rev. B **64**, 020501(R) (2001).
 [14] K.P. Bohnen, R. Heid and B. Renker, Phys. Rev. Lett. **86**, 5771 (2001).
 [15] J.Hlinka *et al.*, Phys. Rev. B **64**, 140503(R) (2001).
 [16] J.W. Quilty *et al.*, Phys. Rev. Lett. **88**, 087001 (2002).
 [17] H. Martinho *et al.*, Solid State Comm. **125**, 499 (2003).
 [18] Y.G. Naidyuk, *et al.*, Phys. Rev. Lett. **90**, 197001 (2003).
 [19] S.Narasimhan, and D.Vanderbilt Phys. Rev. B **43**, 4541 (1991); A. Debernardi, S. Baroni and E. Molinari Phys. Rev. Lett. **75**, 1819 (1995); G. Lang *et al.*, Phys. Rev. B **59**, 6182 (1999).
 [20] P. Hohenberg and W. Kohn, Phys. Rev. **136B**, 864 (1964); W. Kohn and L.J. Sham, Phys. Rev. **140A**, 1133 (1965).
 [21] P. Giannozzi *et al.*, Phys. Rev. B **43**, 7231 (1991); S. Baroni *et al.*, Rev. Mod. Phys. **73**, 515 (2001).
 [22] M. Lazzeri and S. de Gironcoli, Phys. Rev. B **65**, 245402 (2002).
 [23] W. Jones and N.H. March, *Theoretical Solid state Physics* (Dover Publications, New York, 1975) Volume 1, Appendix A3.7.5.
 [24] J. Menendez, and M. Cardona, Phys. Rev. B **29**, 2051 (1984).
 [25] The calculation of the tadpole diagram involves a sum of the type $\sum_{\mathbf{q}, j_2} V^{(3)}(0j_1, -\mathbf{q}j_2, \mathbf{q}j_2)$. Such an object transforms as a first order tensor (*e.g.* as a force) with respect to the crystal symmetries. Consequently, in MgB_2 , where atomic positions are fixed by symmetry, it is zero.
 [26] N. Troullier and J.L. Martins, Phys. Rev. B **43**, 1993 (1991); S.G. Louie, S. Froyen, and M.L. Cohen, Phys. Rev. B **26**, 1738 (1982). For Mg we used nonlinear core corrections and we treated 2s and 2p levels as core states.
 [27] We use the room temperature structure of [11], and extrapolating the $T=0$ K one according to the experimental thermal expansion of Ref. [28]. Third and fourth order derivatives of the energy are computed on a $4 \times 4 \times 2$ mesh of phonon \mathbf{q} -points in the BZ corresponding to the $1 \times 1 \times 1$ cell, and Fourier interpolated at the \mathbf{q} -points of the thicker (20^3) grid used for the summation in Eq. 2. Other computational details are the same as in Ref. [11].
 [28] J.D. Jorgensen, D.G. Hinks, and S. Short, Phys. Rev. B **63**, 224522 (2001).
 [29] J.P. Perdew, K. Burke, and M. Ernzerhof, Phys. Rev. Lett. **77**, 3865 (1996).
 [30] J.P. Perdew and A. Zunger, Phys. Rev. B **23**, 5048 (1981).
 [31] The $14 \times 14 \times 8$ grid is used to compute only $V^{(3)}$ and $V^{(4)}$. While computing the shifts from Eqs. 2, we always use frequencies calculated using the well converged 16×16 electronic integration grid.